Journal of Applied Polymer Science

Estimation of the mechanical properties of urea–formaldehyde microcapsules by compression tests and finite element analysis

Wanpeng Ma, Wei Zhang, Yang Zhao, Sijie Wang
Science and Technology on Remanufacturing Laboratory, Academy of Armored Forces Engineering, Beijing 100072, China
Correspondence to: W. Zhang (E-mail: zhangwei18@hotmail.com)

ABSTRACT: Information on the mechanical properties of microcapsules is essential to understanding their performance during manufacturing, processing, and applications. The mechanical properties of urea–formaldehyde (UF) microcapsules filled with ethyl phenyl acetate (EPA) were determined by applying single-microcapsule compression and a finite element model. Microcapsules were prepared by in situ polymerization, and the average wall thickness of microcapsules was 192 ± 12 nm as determined using scanning electron microscopy. The deformation behavior of the microcapsule was measured by a single-microcapsule compression experiment between two parallel plates. The results show that both burst deformation and burst force were linearly related to microcapsule size. A model for an elastic shell filled with incompressible fluid was used to simulate compression of the microcapsule in ABAQUS. Dimensionless parameters were introduced to the model. The relationship between dimensionless force and dimensionless displacement depended on the ratio of wall thickness to diameter (ε). However, the relationship remained the same when ε was less than 1% and can be fitted well by the mathematical equation. An estimation of Young's modulus can be obtained from the compression data for the dimensionless deformation from 10% to 15%. The average Young's modulus of a UF/EPA microcapsule is estimated to be 2.12 ± 0.45 GPa. © 2016 Wiley Periodicals, Inc. J. Appl. Polym. Sci. **2016**, *133*, 43414.

KEYWORDS: mechanical properties; membranes; nanostructured polymers; stimuli-sensitive polymers

Received 1 November 2015; accepted 2 January 2016
DOI: 10.1002/app.43414

INTRODUCTION

Microcapsules are widely used to produce functional products in the food industry, agriculture, printing, active coatings, and self-healing materials.[1–5] For instance, the repair process of a self-healing material is triggered by a microcapsule rupturing when a crack propagates through the matrix, followed by the release of a healing agent into the crack plane. Then the healing agent mixes with the catalyst and bonds the crack through polymerization.[4] Information on the mechanical properties of microcapsules is essential to understanding their performance during manufacturing, processing, and applications.

Their mechanical properties define the deformation of microcapsules under external load, which is crucial to ensuring mechanical triggering when material is damaged. Many experimental methods have been developed to investigate the mechanical properties of microcapsules, such as compression, osmotic bursting experiments, micropipette aspiration, poking, fluid shear, and optical tweezers.[6,7] However, most techniques could only measure local mechanical properties at very small deformations. Singe microcapsule compression is a simple way to obtain force and deformation at failure. By solving analytical equations that govern deformation of a spherical shell with an appropriate elastic shell model, extraction of shell material mechanical parameters is possible.[8–10] However, obtaining a theoretical force curve becomes complicated and is rarely performed daily because comparison with theoretical models is time consuming.

Self-healing materials based on ethyl phenyl acetate (EPA) microcapsules could fully restore fracture toughness of epoxy resin (with healing efficiencies up to 100%) and heal fiber/matrix interfacial debone strength and thermoplastics.[11–13] Thus, the mechanical properties of urea–formaldehyde (UF) microcapsules filled with ethyl phenyl acetate were investigated. In this study, a single-microcapsule compression experiment was used to detect the deformation of microcapsules. A model of an elastic membrane filled with liquid was then established. Finally, a simple practical method was proposed to calculate elastic properties from experiments.

MATERIALS AND METHODS

Materials

Urea (AR) and ammonium chloride (AR) were purchased from Tianjin Fengchuan Chemical Reagent Technologies Co., Tianjin, China. Formalin solution (37% formaldehyde in water) and

resorcinol (AR) were purchased from Xilong Chemical Co., Shantou, China. The surfactant ethylene–maleic anhydride (EMA, AR) copolymer was purchased from Sigma-Aldrich, St. Louis, Missouri. Distilled water was used to prepare aqueous solutions. A 5% NaOH solution was used for adjusting pH. Ethyl phenyl acetate (99%, AR) as a healing agent was purchased from Aladdin, Shanghai, China. Chemicals were used without further purification.

Microcapsule Preparation

Microcapsules were synthesized using an in situ polymerization procedure with slight modifications.[14,15] Exactly 1.25 g EMA was mixed with 50 ml deionized water in a warm bath to obtain a 2.5% aqueous surfactant solution. Then, 200 ml of deionized water and 50 ml of 2.5 wt % aqueous solution of EMA were mixed in a 500 ml beaker. The microcapsule wall-forming materials, 5 g urea, 0.5 g ammonium chloride, and 0.5 g resorcinol, were dissolved in the solution and stirred for several minutes. The pH was adjusted to 3.5 by adding the NaOH solution. Then, 90 ml EPA was added into the solution and agitated with an emulsification isotropic machine to form an oil/water emulsion. The diameter of the microcapsule was controlled by the agitation rate. The beaker was suspended in a temperature-controlled water bath and was mixed slowly with a digital mixer (RW20, IKA, Staufen Im Breisgau, Baden-Wurttemberg, Germany). Finally, 12.67 g of 37 wt % aqueous solution of formaldehyde was added into the mixing solution, and the solution was heated to 55°C at a rate of 1°C/min. After 4 hours of continuous heating, the microcapsules were rinsed with deionized water and then separated with a filter and air-dried for several days. The microcapsules were separated into three size ranges with the aid of sieves of 100, 200, and 400 μm: $<$100, 100–200, and 200–400 μm.

Dried microcapsules were mounted on conductive carbon tape and then sputtered with a thin layer of gold–palladium to prevent charging under electron beam. The surface morphology was examined by scanning electron microscopy (SEM, QUANTA200, FEI, Hillsboro, Oregon State) in low-vacuum mode. To measure wall thickness, the microcapsule was ruptured by blade and wall morphology was observed by field-emission SEM (S4800, Hitachi, Tokyo, Japan).

Single-Microcapsule Compression

Capsule compression tests were conducted on a Bose 3100, Eden Prairie, MN. A flat probe about 2 mm in diameter was used and positioned perpendicular to the surface of a glass slide. Then, a small amount of free-flow microcapsules was drawn onto the glass slide. To confirm that only one microcapsule was in contact with the probe, the contact region was first examined using an optical microscope. The flat probe was then moved toward the slide above the single microcapsule, which was observed by the optical microscope. The displacement was applied at a rate of 1 μm/s controlled by a computer. Force data were acquired from a 250 g load cell. The instrument had a force and a displacement resolution of 0.1 mN and 1 nm, respectively. Compression was terminated when the probe touched the slide and the force reached 100 g (enough to burst). The probe then returned to the starting position. The diameter of the microcapsule was calculated from the distance traveled by the probe from the point of a force being detected (microcapsule–probe contact) and the position of the probe eventually touching the slide. Microcapsules of three size ranges ($<$100, 100–200, and 200–400 μm sieved previously) were compressed to determine the mechanical properties.

Finite Element Analysis

To decrease computation and time, only the top left of a microcapsule was modeled. A finite element model was established to simulate the compression of microcapsules using ABAQUS/Standard 6.10. The microcapsule included a UF wall and liquid core material of EPA. The wall of the microcapsule was modeled by 300 axisymmetric shell elements SAX1, where wall thickness (t) was defined as one of the element variables. The EPA was modeled by using FAX2 elements to model coupling between deformation of the microcapsule and pressure exerted by the fluid contained in the microcapsule. FAX2 elements are surface elements sharing nodes at the microcapsule wall with standard elements. A flat probe was modeled by analytical rigid element. Contact between the probe and the microcapsule was assumed to be frictionless and was modeled as contact pairs. Frictional effects were neglected given that the models are idealized. Application of load in the finite element analysis (FEA) models was accomplished by assigning a concentrated load to the flat probe, and the load was displacement-controlled. Since the microcapsule wall was assumed to be incompressible, the Poisson ratio was 0.5. The model was restricted to the linear elastic regime because of the brittle nature of the UF, and, thus, Young's modulus (E) was used as a mechanical parameter of the microcapsule. The diameter of the microcapsule and the wall thickness were considered as the geometric parameters of the capsules in the finite element analysis. Additionally, microcapsules were assumed to be impermeable in the time range in which compressions are made, and thus the volume of EPA was kept constant by setting a type of FAX2 to be hydraulic and specific to incompressible fluid. The density of EPA was 1.03 kg/L^{-1}. In this study, the FEA focused on the effects of varying microcapsule diameter, wall thickness, and Young's modulus on deformation behavior.

RESULTS AND DISCUSSION

Surface Morphology and Wall Thickness

Microcapsules have a rough outer surface characterized by clusters of nanoparticles, as shown in Figure 1. Figure 2 shows that the microcapsules have a smooth inner surface. This particular morphological feature could contribute to the microcapsule formation process.[14] Encapsulation proceeds through liquid–liquid phase separation. Polymerization between urea and formaldehyde is initiated in the water phase. The smooth nonporous inner surface is believed to be the result of the deposition of low-molecular-weight prepolymer at the oil–water interface. As the molecular size increases, UF nanoparticles are deposited at the interface to form this rough surface morphology. This feature improves bonding strength between the microcapsule and the matrix and thus increases the probability of rupturing the capsule. Wall thickness can be measured with SEM by rupturing a microcapsule, as shown by Figure 2; however, the corresponding microcapsule size cannot be measured simultaneously. To investigate the effect of microcapsule size on wall thickness, 10

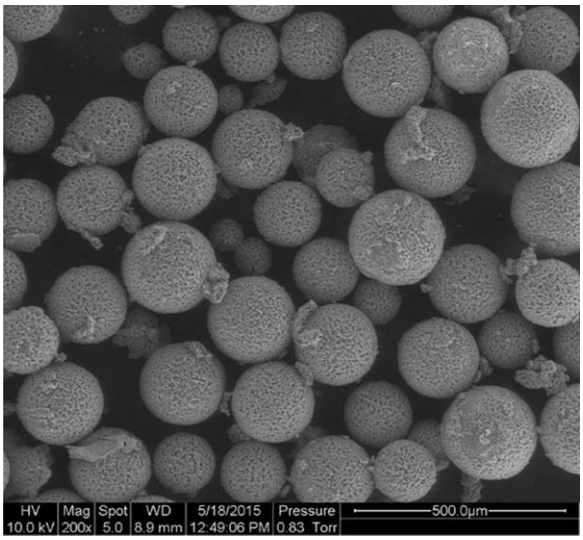

Figure 1. Surface morphology of UF/EPA microcapsules.

microcapsules each of three size ranges (<100, 100–200, and 200–400 μm sieved previously) were measured. Figure 3 shows that wall thickness is independent of capsule size, and the average value is 192 ± 12 nm. Therefore, the wall thickness of the microcapsules is assumed to be constant regardless of microcapsule size because they are from the same preparation batch.

Relationship between Force and Displacement

A typical force–displacement curve from the compression measurements is shown in Figure 4. As the probe moved toward the microcapsule until it touched point A, the force imposed on the microcapsule increased with displacement. When the microcapsule was compressed to point B, the force quickly reduced to point C, due to rupture of the microcapsule and release of the core material. The microcapsule shell wall did not buckle and remained effectively intact after rupture. Similar results have been obtained for UF microcapsules.[8,16] The force and displacement at point B were defined as burst force and burst deformation, respectively. Burst force and burst deformation were 4.9 mN and 38.6 μm, respectively. After rupture, the broken microcapsule was further compressed, resulting in a second cracking of the ruptured wall, which was indicated by peak point C'. On further motion, the probe touched (point D) the slide and the force rose rapidly. The microcapsule can be calculated using the displacement from points A to D. Thus, the diameter of the microcapsule under test is 153 μm. The relationship between force and displacement from points A to B was important to determine intrinsic parameters, such as Young's modulus, as described below.

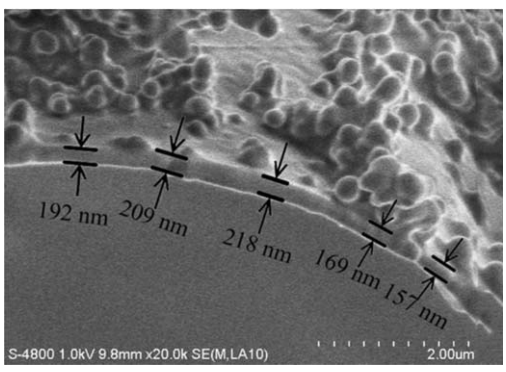

Figure 2. Wall thickness measured by SEM after rupturing microcapsules.

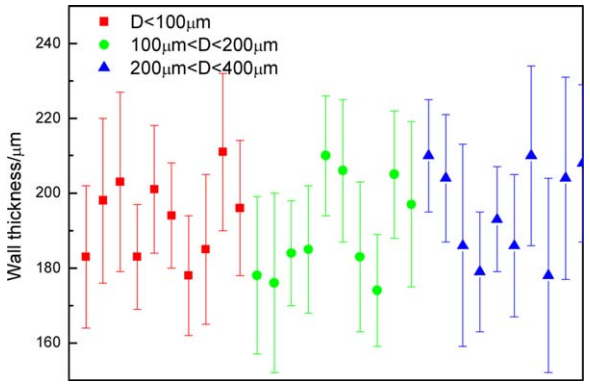

Figure 3. Wall thickness measured with SEM. Microcapsules were separated into three size ranges: <100, 100–200, and 200–400 μm. [Color figure can be viewed in the online issue, which is available at wileyonlinelibrary.com.]

Figure 5 shows force–displacement curves for different microcapsule sizes displaying different profiles. Smaller capsules were stiffer than larger ones because of larger relative wall thickness, which could be characterized by the ratio of wall thickness to diameter (ε). For example, ε for a 50 μm microcapsule was 0.384%, and for a 200 μm microcapsule it was 0.096%, given that the average wall thickness was 192 nm. The results show an increase in the stiffness with increasing ε. Burst deformation seemed to be linear with the microcapsule size, as shown in Figure 6. The dependence of burst deformation on capsule size has been observed previously,[17] and burst force follows the same rule. To investigate this linear relationship, normalized burst deformation is defined as the ratio of burst deformation to diameter. Figure 7 shows that the normalized burst deformation holds constant at $25.2 \pm 7.9\%$ for different microcapsule sizes. The normalized burst deformation is related to the wall-forming material, core material, and preparation method. This value is 25% for the UF/EPA microcapsule in this experiment, 70% for an melamine-formaldehyde (MF) microcapsule,[18] and

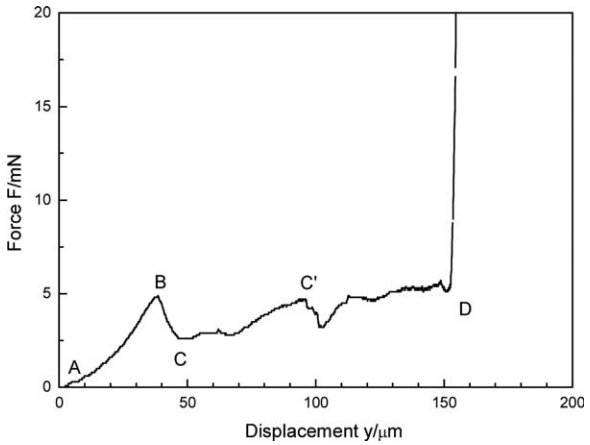

Figure 4. Typical force–displacement curve from the single-microcapsule compression tests.

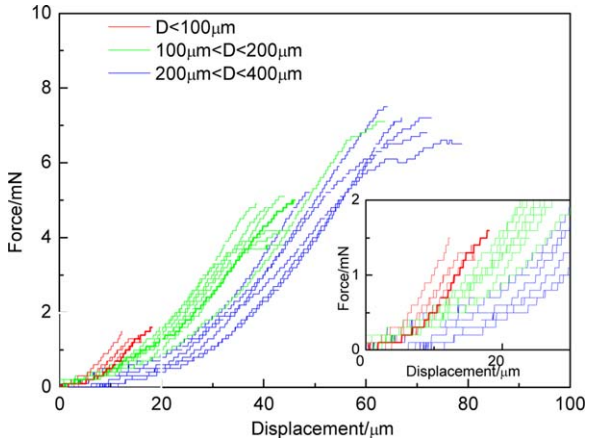

Figure 5. Force–displacement curves for different microcapsule sizes. [Color figure can be viewed in the online issue, which is available at wileyonlinelibrary.com.]

45% for UF/dicyclopentadiene (DCPD) microcapsules.[8] Similarly, normalized burst force is defined as the ratio of burst force to diameter; the unit of normalized force is N m^{-1}. The average value of normalized burst force is 24.8 ± 7.5 N m^{-1} for different microcapsule sizes.

Finite Element Simulations of Microcapsule Compression with Different Thickness Ratios

The deformation behavior of a microcapsule is dependent on E, wall thickness t, and diameter of the microcapsule D. Inspired by normalized deformation and normalized force, dimensionless parameters are defined as simply following the deformation model[19,20]:

$$\text{Dimensionless force } \bar{F} = \frac{F}{EtD} \tag{1}$$

$$\text{Dimensionless displacement } \bar{y} = \frac{y}{D} \tag{2}$$

$$\text{Ratio of wall thickness to diameter } \varepsilon = \frac{t}{D} \tag{3}$$

Figure 8(a) shows the plot of dimensionless force and dimensionless displacement for different t/D ratios (ε) from 0.1% to 10%.

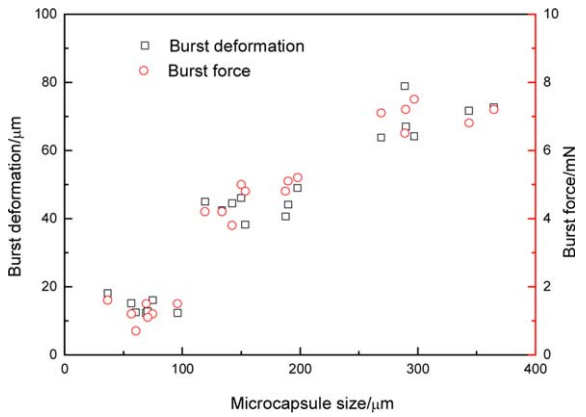

Figure 6. Burst deformation and burst force for different microcapsule sizes. [Color figure can be viewed in the online issue, which is available at wileyonlinelibrary.com.]

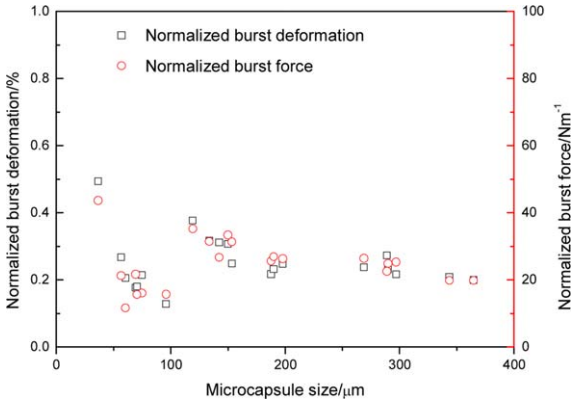

Figure 7. Normalized burst deformation and normalized burst force for different microcapsule sizes. [Color figure can be viewed in the online issue, which is available at wileyonlinelibrary.com.]

For the same ε, the $\bar{F} - \bar{y}$ curve keeps the same profiles contributing to the similarity principle. Microcapsules with different ε have different force profiles, which indicate the relevance of the bending effect. Also, $\bar{y}$ becomes small for a given $\bar{F}$ with large ε, suggesting that microcapsules have higher stiffness with a thicker wall. When ε is smaller than 1%, dimension force profiles almost overlap. The microcapsule wall is then considered to be a thin shell, and the transverse shear flexibility can be overlooked. For a UF/EPA microcapsule, the average wall thickness is 192 nm, and the size of the microcapsule falls within the range 40–200 μm, so ε is 0.08–0.44%. Since $\varepsilon < 1\%$ for the microcapsule, the effect of ε on microcapsule deformation can be ignored, and the dimensionless curves follow the same rule.

To determine the elastic property of microcapsules, the relationship between dimensionless parameters $\bar{F}$ and $\bar{y}$ was fitted by a mathematical equation. FEA results are transformed into a natural logarithm value. As shown in Figure 8(b), $\ln(\bar{F})$ aligns well with $\ln(\bar{y})$ and is fitted by using the least squares method, and R^2 is 99.997%. Therefore,

$$\ln(\bar{F}) = 0.14968 + 1.93451 \times \ln(\bar{y}). \tag{4}$$

According to eqs. (1) and (2), the relationship between force and displacement can be expressed as

$$F = 1.1615\left(\frac{y}{D}\right)^{1.93451} EtD \tag{5}$$

According to Reissner,[21–23] applied force F is linear with the resulting deformation y:

$$F = \frac{t^2}{R}\frac{4E}{\sqrt{3(1-\nu^2)}}y \tag{6}$$

where R is the radius of the microcapsule and ν is the Poisson ratio. In this study, ν is supposed to be 0.5. The finite element model result compared with eq. (6) for ε is 0.1% and 5% at small deformation, as shown in Figure 9. The FEA simulation shows that the force is linear with displacement for a thick microcapsule ($\varepsilon = 5\%$), which is in accordance with Reissner's prediction. However, deviation between eq. (6) and FEA simulation became large for $\varepsilon = 0.1\%$. This finding suggests that Reissner's theory may fail to predict the mechanical properties of thin-walled microcapsules at high deformation.

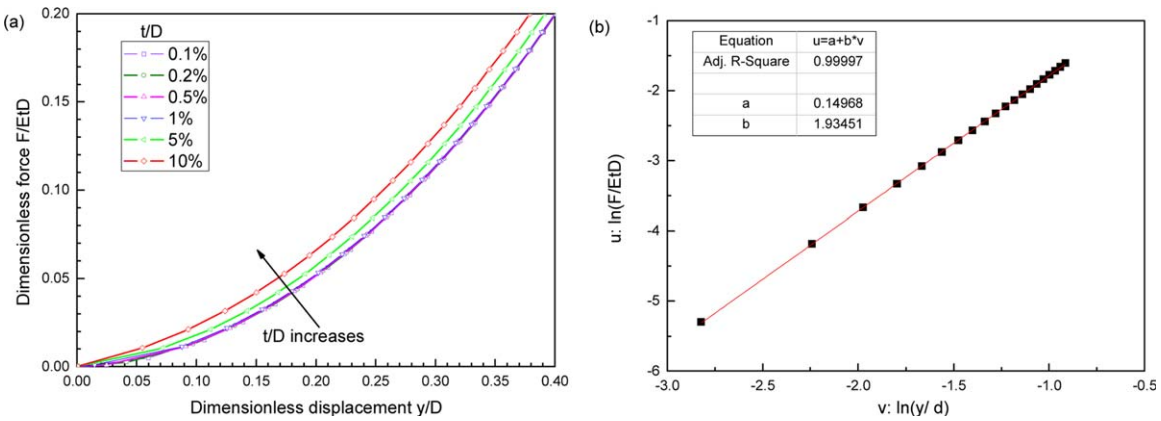

Figure 8. Finite element analysis results: (a) dimensionless force–dimensionless displacement curves for different t/D ratios from 0.1% to 10%; (b) linear fit of ln $\bar{F}$ and ln $\bar{y}$ by the least squares method. [Color figure can be viewed in the online issue, which is available at wileyonlinelibrary.com.]

Therefore, Young's modulus for thin-walled microcapsules at high deformation can be calculated:

$$E(y)=\frac{F}{1.1615\left(\frac{y}{D}\right)^{1.93451}tD} \tag{7}$$

This method can be applied to evaluate mechanical properties when the t/D ratio is smaller than 5%. Given that the wall thickness of the microcapsule can be measured by SEM, E can be absolutely estimated from the compression data.

Determination of Elastic Mechanical Property

Figure 10 shows the calculation results of E according to eq. (7) for the microcapsule corresponding to Figure 4. The results show that E fluctuates greatly when $\overline{y}$ is smaller than 10% because both force and displacement are small such that the error of E is big. When $\overline{y}$ is bigger than 20%, E declines slightly, indicating a plastic effect. Therefore, E is calculated for experiment curves for the $\overline{y}$ value from 10% to 15% for many conditions. This range is large enough to avoid errors, but is not too large for nonelastic effects to be relevant. At the same time, this range has sufficient data to compare with the theoretical equation, hence increasing the certainty of estimation.

The E value for a 153 μm UF/EPA microcapsule is estimated to be 2.33 GPa by using this method. The simulation according to eq. (5) fits well with the compression results before the yield point, as shown in Figure 10. When dimensionless displacement is larger than 23%, the deviation between simulation and experiment curves becomes large due to the plastic effect.[24] For large deformations, the plastic effect is not negligible, so E would not remain constant and may be overestimated. The modified E method after the yield point is dependent on which plastic model should be used and needs further research in our future work.

The estimated E is shown in Figure 11 for different microcapsule sizes. The average value is 2.12 ± 0.45 GPa, and the wall thickness is constant (192 nm) for estimation. The scatter plot of E is large, which may be due to wall thickness and the plastic effect. According to eq. (7), E has a negative relationship with t, so E is sensitive to wall thickness variation. Variation in wall thickness alters the estimated E value by the same percentage.

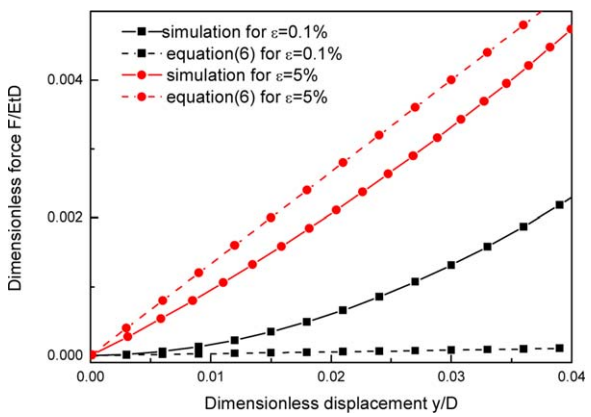

Figure 9. Comparison between finite element analysis result and Reissner's theory for ε of 0.1% and 5%, respectively. [Color figure can be viewed in the online issue, which is available at wileyonlinelibrary.com.]

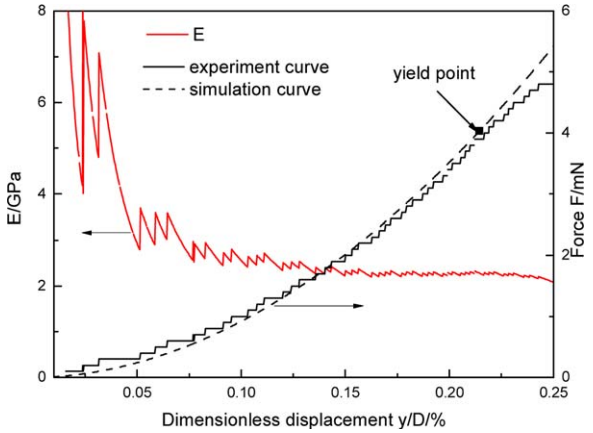

Figure 10. Plot of E versus y/d and comparison of force–displacement curve for experiment and simulation results. [Color figure can be viewed in the online issue, which is available at wileyonlinelibrary.com.]

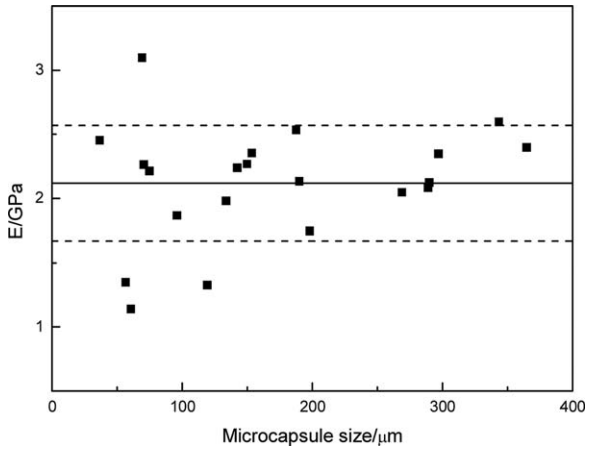

Figure 11. Estimation of *E* for different microcapsule sizes.

CONCLUSIONS

An easy approach to estimating the elastic mechanical properties of microcapsules is proposed by using a finite element model. UF microcapsules filled with EPA were prepared by in situ polymerization. A single-microcapsule compression experiment was used to investigate the deformation of UF microcapsules. The results indicated that burst deformation and burst force are linearly related to microcapsule size. A model for an elastic shell filled with incompressible fluid was used to simulate the compression of the microcapsule. The effect of ε on microcapsule deformation can be ignored when ε is less than 1%. The relationship between dimensionless force and dimensionless displacement can be fit well with a mathematical equation. Given that the wall thickness of the microcapsule can be measured by SEM, an estimation of Young's modulus can be obtained from the compression data. To avoid error and the nonelastic effect, Young's modulus was calculated for dimensionless deformation from 10% to 15%. The average Young's modulus of a UF/EPA microcapsule is estimated to be 2.12 ± 0.45 GPa. This method is valid and feasible for determining the mechanical properties of thin-walled microcapsules at large deformation.

ACKNOWLEDGMENTS

The work was supported by the National Natural Science Foundation of China (grant no. 50775222) and the Equipment Repair and Reformation Program, China (Grant 2014WG13).

REFERENCES

1. Champagne, C. P.; Fustier, P. *Curr. Opin. Biotechnol.* **2007**, *18*, 184.
2. Sopena, F.; Maqueda, C.; Morillo, E. *Cienc. Invest. Agrar.* **2009**, *36*, 27.
3. Suryanarayana, C.; Rao, K. C.; Kumar, D. *Prog. Org. Coat.* **2008**, *63*, 72.
4. White, S. R.; Sottos, N.; Geubelle, P.; Moore, J.; Kessler, M. R.; Sriram, S.; Brown, E.; Viswanathan, S. *Nature* **2001**, *409*, 794.
5. White, S. R.; Moore, J. S.; Sottos, N. R.; Krull, B. P.; Cruz, W. A. S.; Gergely, R. C. R. *Science* **2014**, *344*, 620.
6. Neubauer, M. P.; Poehlmann, M.; Fery, A. *Adv. Colloid Interface Sci.* **2014**, *207*, 65.
7. Su, J.; Ren, L.; Wang, L. *Colloid. Polym. Sci.* **2005**, *284*, 224.
8. Keller, M. W.; Sottos, N. R. *Exp. Mech.* **2005**, *46*, 725.
9. Liu, K. K. J. *Phys. D. Appl. Phys.* **2006**, *39*, R189.
10. Rachik, M.; Barthes-Biesel, D.; Carin, M.; Edwards-Levy, F. *J. Colloid Interface Sci.* **2006**, *301*, 217.
11. Caruso, M. M.; Blaiszik, B. J.; White, S. R.; Sottos, N. R.; Moore, J. S. *Adv. Funct. Mater.* **2008**, *18*, 1898.
12. Blaiszik, B. J.; White, S. R.; Sottos, N. R.; Jones, A. R. *Compos. Sci. Technol.* **2013**, *79*, 1.
13. Celestine, A.-D. N.; Sottos, N. R.; White, S. R. *Polymer* **2015**, *69*, 241.
14. Brown, E. N.; Kessler, M. R.; Sottos, N. R.; White, S. R. *J. Microencapsulation* **2003**, *20*, 719.
15. Blaiszik, B. J.; Caruso, M. M.; McIlroy, D. A.; Moore, J. S.; White, S. R.; Sottos, N. R. *Polymer* **2009**, *50*, 990.
16. Sun, G.; Zhang, Z. *Int. J. Pharm.* **2002**, *242*, 307.
17. Zhang, Z.; Saunders, R.; Thomas, C. R. *J. Microencapsulation* **1999**, *16*, 117.
18. Pretzl, M.; Neubauer, M.; Tekaat, M.; Kunert, C.; Kuttner, C.; Leon, G.; Berthier, D.; Erni, P.; Ouali, L.; Fery, A. *ACS Appl. Mater. Interfaces* **2012**, *4*, 2940.
19. Liu, T. Z. *Chinese J. Proc. Eng.* **2005**, *5*, 450.
20. Mercadé-Prieto, R.; Nguyen, B.; Allen, R.; York, D.; Preece, J. A.; Goodwin, T. E.; Zhang, Z. *Chem. Eng. Sci.* **2011**, *66*, 2042.
21. Reissner, E. J. *Math. Phys.* **1946**, *25*, 80.
22. Reissner, E. J. *Math. Phys.* **1946**, *25*, 279.
23. Reissner, E. J. *Math. Mech.* **1958**, *7*, 121.
24. Mercadé-Prieto, R.; Allen, R.; York, D.; Preece, J. A.; Goodwin, T. E.; Zhang, Z. *Chem. Eng. Sci.* **2011**, *66*, 1835.